

# Kinetic Study by FTIR, TMA, and DSC of the Curing of a Mixture of DGEBA Resin and $\gamma$ -Butyrolactone Catalyzed by Ytterbium Triflate

Xavier Ramis,<sup>1</sup> Josep Maria Salla,<sup>1</sup> Cristina Mas,<sup>2</sup> Ana Mantecón,<sup>2</sup> Angels Serra<sup>2</sup>

<sup>1</sup>Departament de Màquines i Motors Tèrmics, Universitat Politècnica de Catalunya, Av. Diagonal 647, 08028 Barcelona, Spain

<sup>2</sup>Departament de Química Analítica i Química Orgànica, Universitat Rovira i Virgili, Plaça Imperial Tàrraco 1, 43005 Tarragona, Spain

Received 16 May 2003; accepted 30 July 2003

**ABSTRACT:** A mixture of diglycidylether of bisphenol A (DGEBA) and  $\gamma$ -butyrolactone ( $\gamma$ -BL) was cured in the presence of ytterbium triflate as a catalyst. The kinetics of the various elemental processes that occur in the curing process were studied by means of isothermal curing in the FTIR spectrometer. The kinetics of the contraction during the curing was also evaluated by TMA. In both cases, the kinetics was analyzed by means of isoconversional procedure and the kinetic model was determined with the so-called compensation effect (isokinetic relationship). The isothermal

kinetic analysis was compared with that obtained by dynamic curing in DSC. We found that all the reactive processes and the contraction follow a surface-controlled reaction type of kinetic mechanism,  $R_3$ . © 2004 Wiley Periodicals, Inc. *J Appl Polym Sci* 92: 381–393, 2004

**Key words:** FTIR; thermomechanical analysis (TMA); differential scanning calorimetry (DSC); kinetics (polym.); curing of polymers

## INTRODUCTION

The curing of thermosetting materials is generally accompanied by shrinkage because covalent bonds form between chains and increase the density of the materials. This shrinkage leads to internal stress in the material, reduces adhesion to the substrate, and produces microvoids and microcracks, which reduce the durability of the material.<sup>1,2</sup>

Shrinkage during curing could be reduced or eliminated using monomers that polymerize without contraction or even with expansion. Ring-opening polymerization leads to less shrinkage than that produced by polycondensation or polyaddition, because not only are small molecules not eliminated in the polymerization, but for every bond that changes from a van der Waals distance to a covalent distance, another bond changes from a covalent distance to a near van

der Waals distance. Thus, the ring-opening polymerization of bicyclic monomers [spiroorthoesters (SOEs) or spirocarbonates (SOCs), etc.] is a good strategy for obtaining nonshrinkable resins that can be applied in adhesives, coatings, or composites.<sup>3,4</sup>

The classical synthetic procedure for obtaining SOEs is to react lactones with epoxides in the presence of a Lewis acid as a catalyst.<sup>5</sup> In this way, cationic crosslinking of mixtures of epoxy resins with lactones could take place with little shrinkage because SOE groups are formed during this process.<sup>6</sup>

Lanthanide triflates are Lewis acids that can act as catalysts in the cationic curing of epoxy resins.<sup>7,8</sup> These compounds are commercially available and maintain their catalytic activity even in aqueous solution. Lanthanide ions have low electronegativities and strong oxophilicities, which make it possible for the metal to coordinate to the oxygens in the substrate.

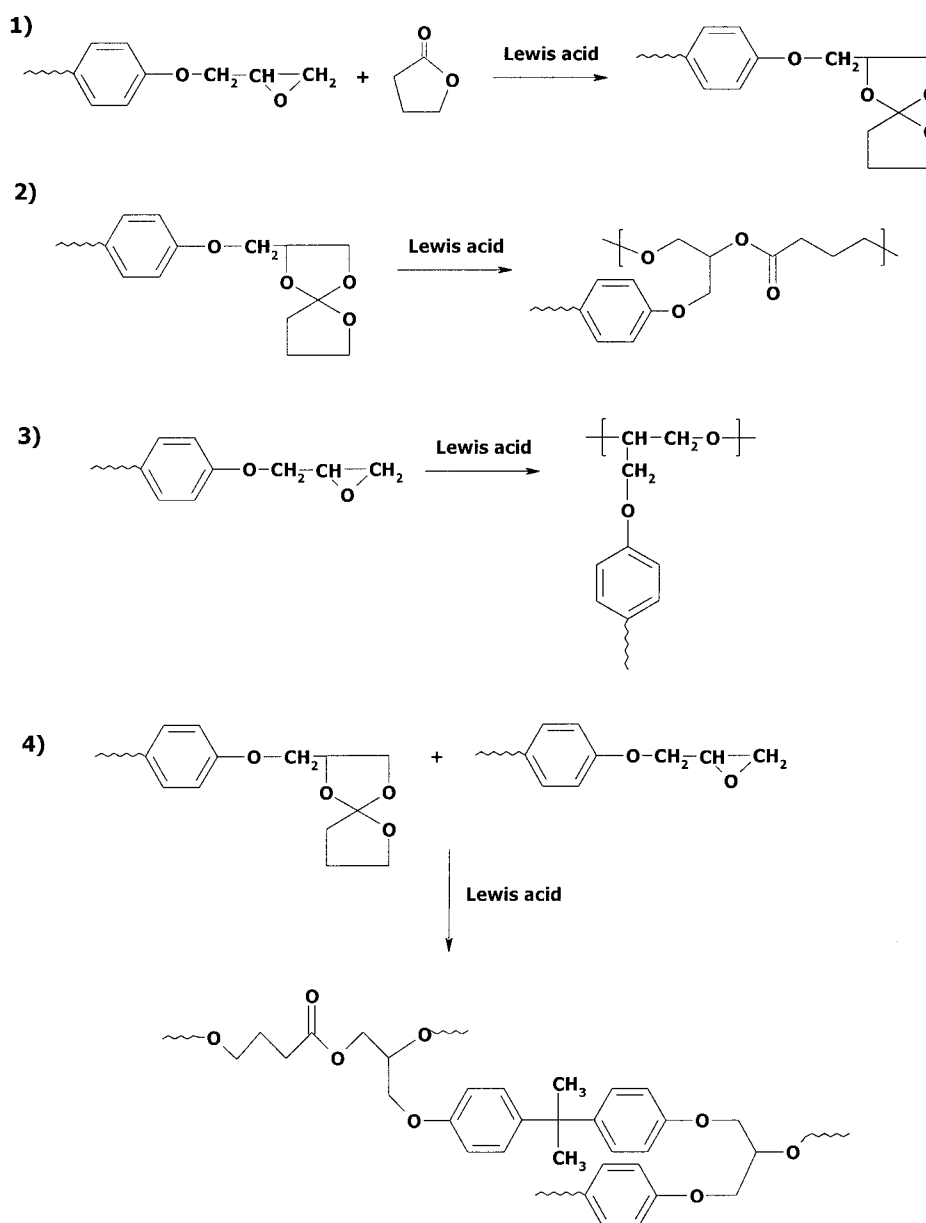
In a previous study<sup>9</sup> we polymerized diglycidylether of bisphenol A (DGEBA) with  $\gamma$ -butyrolactone ( $\gamma$ -BL) using ytterbium triflate as a catalyst. By means of thermomechanical analysis (TMA), we proved that adding  $\gamma$ -BL to the DGEBA leads to materials with low contraction after gelation and therefore with few internal stresses.<sup>1</sup> This was attributed to the initial formation of SOE groups and their polymerization in the last stages of the curing process. Using FTIR we showed that there were four elemental reactive processes: (1) formation of SOE by reaction of

Correspondence to: J. Salla (salla@mmt.upc.es).

Contract grant sponsor: Comisión Interministerial de Ciencia y Tecnología (CICYT); contract grant numbers: MAT2000-1002-C02-02, PPQ2001-2764-C03-02, and MAT2002-00291.

Contract grant sponsor: FEDER; contract grant numbers: PPQ2001-2764-C03-02 and MAT2002-00291.

Contract grant sponsor: Comissió Interdepartamental de Recerca i Innovació Tecnològica (CIRIT); contract grant number: SGR 00318.



Scheme 1

DGEBA with  $\gamma$ -BL, (2) homopolymerization of SOE, (3) homopolymerization of epoxy groups, and (4) copolymerization of SOE and epoxy groups. These elemental processes are represented in **Scheme 1**.

It is not easy to study the isothermal curing of DGEBA with  $\gamma$ -BL and ytterbium triflate by differential scanning calorimetry (DSC). At high temperatures the curing is fast and some heat is evolved before the device stabilizes. At low temperatures the heat is evolved slowly and it cannot be assumed that this heat is accurately evaluated because of the sensitivity of the device.

Dynamic DSC experiments can be performed to obtain kinetic parameters, which make it possible to simulate the behavior during the isothermal curing.<sup>10</sup>

However, DSC gives information only about the overall process but not about the elemental reactions that occur during curing.

Another interesting alternative is to monitor isothermal curing by means of FTIR spectroscopy. In this case, detailed information about the curing process can be obtained by determining the evolution of the absorption bands of the carbonyl and epoxide groups.<sup>6</sup> This method gives the conversion–time ( $\alpha$ – $t$ ) plot at several temperatures for the different reactive groups that change during the curing process. From these plots, using integral isoconversional analysis, activation energy and a second parameter, which is related to the preexponential factor and the degree of conversion, can be calculated. The dependency of the

activation energy ( $E$ ) on the degree of conversion makes it difficult to determine the other two parameters of the kinetic triplet: preexponential factor  $A$  and the function of conversion degree  $g(\alpha)$ . Moreover, because it is not possible experimentally to evaluate the conversion rate ( $d\alpha/dt$ ) by FTIR spectroscopy, the kinetic model [differential function of the degree of conversion  $f(\alpha)$ ] cannot be determined by regression.

The present study focuses on the kinetic analysis of the curing of mixtures of DGEBA with  $\gamma$ -BL using ytterbium triflate as a catalyst. We studied the kinetics of the elemental processes that are part of the curing by FTIR spectroscopy and the overall curing kinetics by DSC. We also used TMA to study the kinetics associated with the shrinkage process. Finally, we propose a method that uses the isoconversional isothermal parameters determined by FTIR or by TMA and the compensation effect<sup>11-13</sup> to determine the complete kinetic triplet. The results were compared with those obtained by nonisothermal procedures.

## EXPERIMENTAL

### Materials

DGEBA (epoxy equiv. = 187 g/eq) (Shell, Tarragona, Spain) and  $\gamma$ -BL (Aldrich, Milwaukee, WI) were used as received. Ytterbium (III) trifluoromethanesulfonate (Aldrich) was used without purification.

### Preparation of the curing mixtures

The mixture was prepared by dissolving 1 phr (one part per hundred parts of mixture, w/w) of ytterbium triflate in 0.01 mol of  $\gamma$ -BL and adding 0.02 mol of DGEBA with magnetic stirring. The prepared sample was kept at  $-18^\circ\text{C}$  before use.

### FTIR spectroscopy

The isothermal curing process, between 100 and  $150^\circ\text{C}$ , was monitored with a FTIR Bomem Michelson MB 100 spectrophotometer (Quebec, Canada) with a resolution of  $4\text{ cm}^{-1}$  in the absorbance mode. An attenuated total reflection accessory with thermal control and a diamond crystal (Golden Gate Heated Single Reflection Diamond ATR, Specac-Teknokroma, Barcelona, Spain) was used to determine FTIR spectra. The disappearance of the absorbance peak at  $915\text{ cm}^{-1}$  (epoxy bending) was used to monitor the epoxy conversion. The consumption of the reactive carbonyl group in  $\gamma$ -butyrolactone was evaluated by measuring the changes in absorbance at  $1773\text{ cm}^{-1}$  (carbonyl C=O stretching of cyclic ester). The appearance of the peak at  $1736\text{ cm}^{-1}$  (carbonyl C=O stretching of aliphatic linear ester), which does not exist in the sample before curing, indicates that ring-opening polymeriza-

tion occurred in SOE. Thus, the latter was used to evaluate the SOE conversion. The peak at  $1509\text{ cm}^{-1}$  (phenyl group) was chosen as an internal standard. After full cure, the peaks at  $915$  and  $1773\text{ cm}^{-1}$  disappeared completely and the peak at  $1736\text{ cm}^{-1}$  reached its maximum height. Absorbances were calculated in terms of peak areas. Conversions of the different reactive groups, epoxide,  $\gamma$ -BL, and SOE, were determined by the Lambert-Beer law from the normalized changes of absorbance at  $915$ ,  $1773$ , and  $1736\text{ cm}^{-1}$  as<sup>6,9,14</sup>

$$\alpha_{\text{epoxy}} = 1 - \left( \frac{\bar{A}_{915}^t}{\bar{A}_{915}^0} \right)$$

$$\alpha_{\gamma\text{-BL}} = 1 - \left( \frac{\bar{A}_{1773}^t}{\bar{A}_{1773}^0} \right) \quad \alpha_{\text{SOE}} = \left( \frac{\bar{A}_{1736}^t}{\bar{A}_{1736}^\infty} \right) \quad (1)$$

where  $\bar{A}^0$ ,  $\bar{A}^t$ , and  $\bar{A}^\infty$  are the normalized absorbance of the reactive group before curing, after reaction time  $t$ , and after complete curing ( $\bar{A}_{915}^0 = A_{915}^0/A_{1509}^0$ ;  $\bar{A}_{1773}^0 = A_{1773}^0/A_{1509}^0$ ;  $\bar{A}_{915}^t = A_{915}^t/A_{1509}^t$ ;  $\bar{A}_{1773}^t = A_{1773}^t/A_{1509}^t$ ;  $\bar{A}_{1736}^t = A_{1736}^t/A_{1509}^t$ ;  $\bar{A}_{1736}^\infty = A_{1736}^\infty/A_{1509}^\infty$ ).

### Thermomechanical analysis

Thermomechanical analysis was carried out in a nitrogen atmosphere using a Mettler-Toledo TMA40 (Greifensee, Switzerland) coupled to a TA4000 thermoanalyzer. The shrinkage,  $\Delta L = L_t - L_o$ , of the resin during curing was measured by applying a force of 0.01 N. The samples impregnated in a silanized fiberglass support were placed between two  $\text{Al}_2\text{O}_3$  discs. Isothermal curing was carried out for different times at temperatures between 110 and  $150^\circ\text{C}$ . The degree of shrinkage in TMA was calculated as<sup>9,10</sup>

$$\alpha_{\text{TMA}} = \frac{L_t - L_o}{L_\infty - L_o} \quad (2)$$

where  $L_o$ ,  $L_t$ , and  $L_\infty$  are the thicknesses of the sample at the onset, at time  $t$ , and upon completion of the reactive process when the material is fully cured, respectively.

### Differential scanning calorimetry

Calorimetric analyses were carried out on a Mettler DSC-821e thermal analyzer using  $\text{N}_2$  as the purge gas in covered aluminum pans. The weight of the samples was approximately 5 mg. Nonisothermal curing was carried out at rates of 2, 5, 10, and  $15\text{ K min}^{-1}$ . In the dynamic curing process the degree of conversion was calculated as

$$\alpha_{DSC} = \frac{\Delta H_T}{\Delta H_{dyn}} \quad (3)$$

where  $\Delta H_T$  is the heat released up to a temperature  $T$ , obtained by integrating the calorimetric signal up to that temperature; and  $\Delta H_{dyn}$  is the total reaction heat associated with complete conversion of all reactive groups. After isothermal FTIR and TMA curing, a dynamic scan was carried out at  $10 \text{ K m}^{-1}$ .

### THEORETICAL

The kinetics of the reaction is usually described by the following rate equation:

$$\frac{d\alpha}{dt} = Af(\alpha) \exp\left(-\frac{E}{RT}\right) \quad (4)$$

where  $t$  is time,  $A$  is the preexponential factor,  $E$  is the activation energy,  $T$  is the absolute temperature,  $R$  is the gas constant, and  $f(\alpha)$  is the differential conversion function.

In general, the kinetic analysis was carried out using an isoconversional method. The basic assumption of these methods is that the reaction rate at constant conversion is only a function of the temperature.<sup>15,16</sup>

#### Isothermal methods

By integrating the rate equation [eq. (4)] in isothermal conditions we obtain

$$\ln t = \ln\left[\frac{g(\alpha)}{A}\right] + \frac{E}{RT} \quad (5)$$

where  $g(\alpha)$  is the integral conversion function, defined as

$$g(\alpha) = \int_0^\alpha \frac{d\alpha}{f(\alpha)} \quad (6)$$

According to eq. (5) the activation energy and the constant  $\ln[g(\alpha)/A]$  can be obtained, respectively, from the slope and the intercept of the linear relationship  $\ln t$  against  $T^{-1}$  for  $\alpha = \text{constant}$ .

#### Nonisothermal methods

By integrating eq. (4) in nonisothermal conditions and reordering it, the so-called temperature integral can be expressed as

$$g(\alpha) = \int_0^\alpha \frac{d\alpha}{f(\alpha)} = \frac{A}{\beta} \int_0^T e^{-(E/RT)} dT \quad (7)$$

where  $\beta$  is the heating rate.

By using the Coats–Redfern<sup>17</sup> approximation to solve eq. (7), and considering that  $2RT/E \ll 1$ , the following equation may be expressed as<sup>18</sup>

$$\ln \frac{g(\alpha)}{T^2} = \ln\left[\frac{AR}{\beta E}\right] - \frac{E}{RT} \quad (8)$$

For a given kinetic model, linear representation of  $\ln[g(\alpha)/T^2]$  against  $T^{-1}$  makes it possible to determine  $E$  and  $A$  from the slope and the ordinate at the origin.

By reordering eq. (8) we can write

$$\ln \frac{\beta}{T^2} = \ln\left[\frac{AR}{g(\alpha)E}\right] - \frac{E}{RT} \quad (9)$$

The linear representation of  $\ln[\beta/T^2]$  against  $T^{-1}$  makes it possible to determine  $E$  and the kinetic parameter  $\ln[AR/g(\alpha)E]$  for every conversion degree. This isoconversional procedure is equivalent to Kissinger's method<sup>19</sup> and similar to Flynn–Wall–Ozawa's method.<sup>20–22</sup>

The constant  $\ln[AR/g(\alpha)E]$  is directly related by  $R/E$  to the constant  $\ln[g(\alpha)/A]$  of the isothermal adjustment [eq. (5)]. Thus, taking the dynamic data  $\ln[AR/g(\alpha)E]$  and  $E$ , and applying eq. (9), we can determine the isoconversional lines [eq. (5)] and simulate isothermal curing.<sup>10,23</sup>

#### Compensation effect (isokinetic relationship)

For complex processes (parallel reactions, successive reactions, physical changes, etc.) it is characteristic for the activation energy and the preexponential factor to depend on the degree of conversion. This generally reflects the existence of a compensation effect through the following equation<sup>10,11,13,22,24–26</sup>:

$$\ln A_\alpha = aE_\alpha + b \quad (10)$$

where  $a$  and  $b$  are constants.

The slope  $a = 1/RT_{iso}$  is related to isokinetic temperature  $T_{iso}$  and the intercept  $b = \ln k_{iso}$  is related to the isokinetic rate constant. Equation (10) represents an isokinetic relationship (IKR), which can be observed as a common point of intersection of the Arrhenius lines (i.e.,  $\ln k$  versus  $T^{-1}$ ) of a series of reactions. This intersection is characterized by a  $k_{iso}$  and a  $T_{iso}$ .

Several authors have suggested that the appearance of the IKR shows that only one reaction mechanism is present and that all reactions have analogous reaction profiles. The existence of more than one IKR or parameters that do not meet the IKR implies that there are different reaction mechanisms.<sup>27,28</sup>

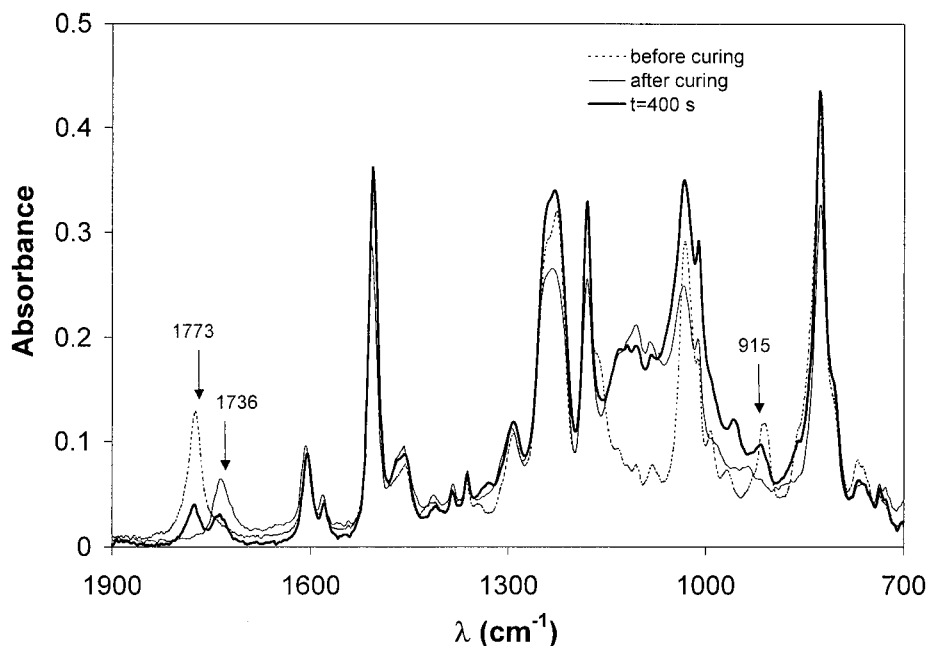


**Figure 1** FTIR spectra of the DGEBA and  $\gamma$ -butyrolactone reactive system catalyzed by 1 phr of ytterbium triflate before, during, and after curing at 150°C.

Isoconversional methods make it possible to determine easily the dependency of  $E$  on the degree of conversion in complex processes (multistep). Vyazovkin<sup>25</sup> proposed a method to obtain, from this information, the two other parameters of the kinetic triplet. Here we have used a similar procedure.

In this study, our aim was to determine the complete kinetic triplet [ $E$ ,  $A$ ,  $g(\alpha)$ ] in systems with  $E = E(\alpha)$ , by using isoconversional kinetic parameters, the slope and intercept of eqs. (5) and (9), and the isokinetic relation, eq. (10). We selected the kinetic model whose IKR has the best linear correlation between the activation energy and preexponential factor.

## RESULTS AND DISCUSSION

Figure 1 shows the FTIR spectra obtained before and after curing the mixture at 150°C. During the curing process there are changes in three absorptions:

1. The carbonyl stretching band of  $\gamma$ -BL at 1773  $\text{cm}^{-1}$  diminishes because  $\gamma$ -BL reacts with the epoxide of the DGEBA resin to form SOE groups.
2. The appearance of a peak at 1736  $\text{cm}^{-1}$ , attributable to a linear aliphatic ester, confirms that ring-opening polymerization of SOE occurs. This process can occur by homopolymerization or by copolymerization with DGEBA. In general, the homopolymerization is less favorable and is important only at the end of curing when there are few epoxide groups.<sup>9</sup>

3. The disappearance of the band at 915  $\text{cm}^{-1}$  associated with the oxirane ring indicates that the epoxide polymerizes. The stoichiometry of the formulation studied (4 eq. of epoxide per 1 eq. of  $\gamma$ -BL) suggests that during curing the epoxide groups take part in the three following reactive processes (in order of importance): homopolymerization of DGEBA, reaction of DGEBA with  $\gamma$ -BL, and copolymerization of DGEBA/SOE.

After curing in the FTIR spectrometer at 150°C, a dynamic scan was always made in the DSC up to 250°C to prove that the curing was complete. In no case was residual enthalpy observed. Then, another dynamic scan was made. The materials before and after the second dynamic scan reached the same  $T_g$  value of about 100°C. At the end of the isothermal crosslinking processes, the absorptions at 1773 and 915  $\text{cm}^{-1}$  totally disappeared and the intensity of the peak at 1736  $\text{cm}^{-1}$  was at its highest. All these considerations led to the conclusion that the material was completely cured isothermally.

Figure 1 shows the partial overlapping between both carbonyl ester absorptions. To quantify the absorptions associated with each carbonyl group, we deconvoluted the spectroscopic signals between 1675 and 1850  $\text{cm}^{-1}$ . To do so we used the curve-fitting method with the Gaussian-Lorentzian sum area function of the program PeakFit (Jandel Scientific Software, San Rafael, CA).<sup>9</sup> Figure 2 shows a representative result for a curing time of 450 s at 150°C. The sum of both deconvoluted peaks perfectly fits the experi-

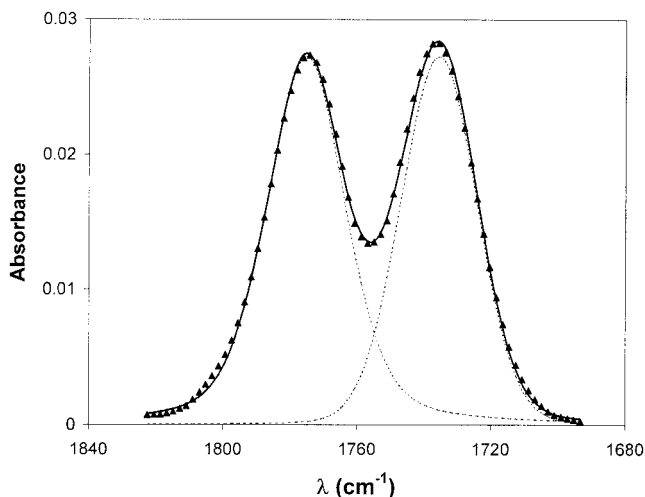


**Figure 2** Carbonyl ester absorptions of the FTIR spectra, representative of the method used to deconvolute both peaks in the DGEBA and  $\gamma$ -butyrolactone reactive system catalyzed by 1 phr of ytterbium triflate and cured at 150°C for 450 s. Symbols are experimental values, dotted lines are the peaks obtained by deconvolution, and the continuous line is the sum of the separated peaks.

mental signal, and the frequency assigned to each signal coincides with the experimental spectrum. Using the deconvoluted peaks of the experimental signals the absorbances were determined by integration and the areas were normalized. The conversions of the reactive species (epoxy,  $\gamma$ -BL, and SOE) were calculated from the normalized absorbances using eq. (1).

Figures 3, 4, and 5 show the degree of conversion of the different reactive species plotted against time at several curing temperatures. We can observe that the curing times of  $\alpha_{\text{epoxy}}$  and  $\alpha_{\gamma\text{-BL}}$  are similar, whereas the times for  $\alpha_{\text{SOE}}$  are longer. This indicates that the reaction between DGEBA and  $\gamma$ -BL and the homopolymerization of DGEBA are similar kinetic processes. The polymerization of SOE takes place more slowly because it depends on the *in situ* formation of SOE. Moreover, at high  $\alpha_{\text{SOE}}$  ( $>0.5$ ) there are few epoxy groups and the homopolymerization of SOE, which is an unfavorable process, is the dominant reaction. The experimental curves in Figures 3, 4, and 5 were used to determine the isoconversional kinetics of each reactive process. By applying eq. (5) at different degrees of crosslinking we obtained the kinetic parameters collected in Table I. In general, the activation energy is higher during the first stages of the curing process and then it diminishes slightly. In some cases, after reaching a minimum value, the activation energy increases. This behavior has already been observed in several thermosetting systems<sup>10,13,29,30</sup> and can be explained by a combination of physical and chemical factors that act during the curing process.

The kinetic parameters of epoxy and  $\gamma$ -BL groups are similar, whereas those of SOE groups are slightly

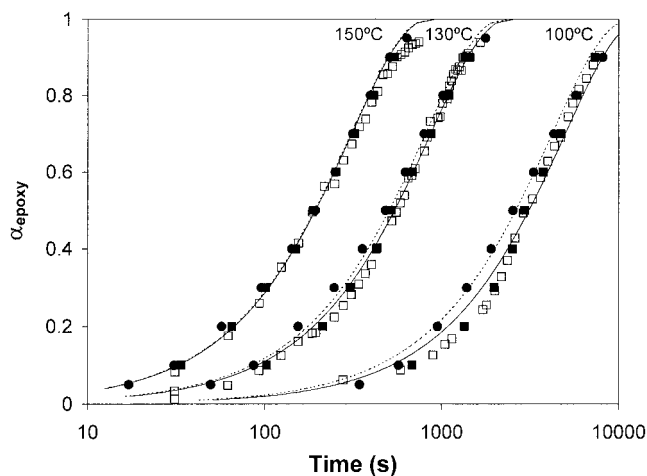


**Figure 3** Plot of the experimental and simulated degrees of epoxy conversion versus curing times for samples cured at different temperatures: ( $\square$ ) experimental isothermal curves; ( $\blacksquare$ ) isoconversional isothermal data obtained by eq. (5); (—) curves obtained by using function  $R_3$  and the isothermal kinetic parameters contained in Table I; ( $\bullet$ ) isoconversional nonisothermal data obtained by eq. (9); (---) curves obtained by using function  $R_3$  and the nonisothermal kinetic parameters in Table IV.

different. Actually, the second parameter  $\ln[g(\alpha)/A]$  is smaller for the SOE group and it leads to longer curing times. However, the activation energies are of the same order of magnitude for all the conversions. This is because the four reactive processes that take place are chemically similar and they all take place by cationic mechanisms. The goodness of the isoconversional analysis used is confirmed by the good regres-

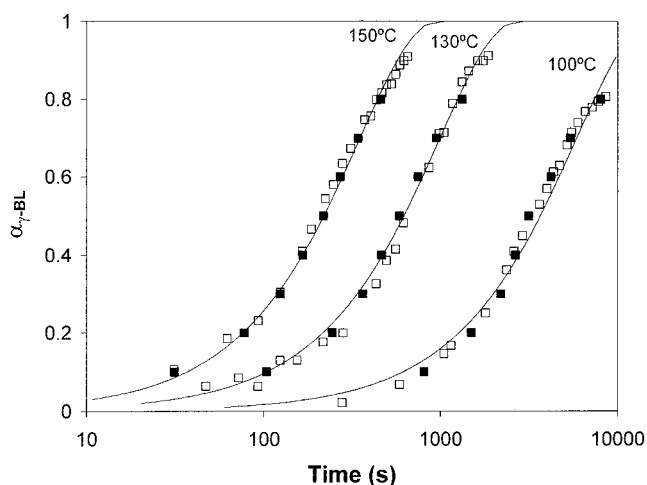


**Figure 4** Experimental and simulated degrees of  $\gamma$ -BL conversion versus curing times for samples cured at different temperatures: ( $\square$ ) experimental isothermal curves; ( $\blacksquare$ ) isoconversional isothermal data obtained by eq. (5); (—) curves obtained by using function  $R_3$  and the isothermal kinetic parameters in Table I.

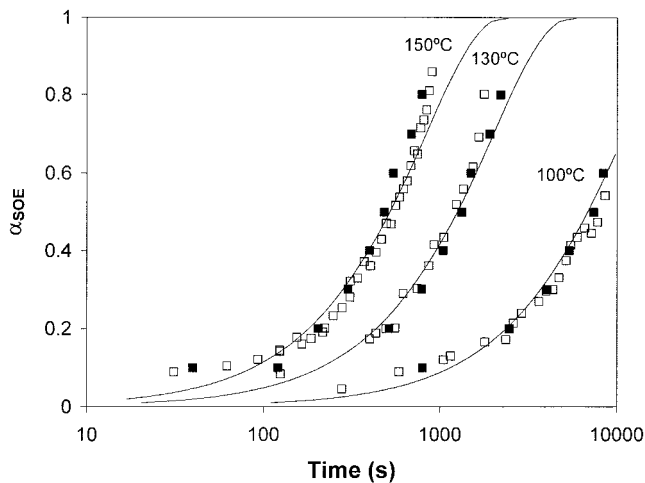


**Figure 5** Experimental and simulated degrees of SOE conversion versus curing times for samples cured at different temperatures: (□) experimental isothermal curves; (■) isoconversational isothermal data obtained by eq. (5); (—) curves obtained by using function  $R_3$  and the isothermal kinetic parameters in Table I.

sion of the isoconversational lines (Table I). Figures 3, 4, and 5 compare the experimental  $\alpha$ - $t$  curves with those obtained from the kinetic parameters given in Table I.

To determine the kinetic model  $g(\alpha)$ , which describes the reactive processes in the curing, we used the isoconversational parameters (Table I) and the isokinetic relationships. From the parameters  $\ln[g(\alpha)/A]$  in Table I we obtained the preexponential factor for the different kinetic models used (see Table II). Then we looked for the isokinetic relationship, eq. (10), for all the models and processes studied. Table III shows the results and the  $T_{iso}$  values determined from the slopes of the IKRs. Although some models have IKR, we considered that for all the reactive processes the  $R_3$  model is the most suitable, given that it has the best regression. In Table I we can see the preexponential factors determined by model  $R_3$ . According to Vyazovkin and Linert,<sup>31</sup> obtaining a  $T_{iso}$  in the experimental temperature range is an indication that the kinetic model accurately describes the reactive process. In our case, for epoxy groups and  $\gamma$ -BL, we obtained a  $T_{iso}$  of 143.8 and 140.3°C, respectively, both in the experimental curing range. However, for the SOE group, we obtained a  $T_{iso}$  of 68.2°C, substantially different from the experimental range. This may be because the polymerization of SOE depends on the quantity of SOE in the reaction medium. This quantity is always limited by the formation of SOE, from DGEBA and  $\gamma$ -BL, and its polymerization.

Figure 6 shows the IKR plots of the reactive species for the  $R_3$  model. As we can see, the kinetics of the epoxy groups and  $\gamma$ -BL is similar (similar IKR) and different (different IKR) for the SOE. In Figures 3, 4, and 5 we plotted the  $\alpha$ - $t$  curves for the  $R_3$  model. For

**TABLE I**  
**Kinetic Parameters of the Curing Obtained by FTIR and TMA for the DGEBA/ $\gamma$ -BL Reactive System Catalyzed by Ytterbium Triflate<sup>a</sup>**

$\alpha$	Epoxy (915 $\text{cm}^{-1}$ )				$\gamma$ -Butyrolactone (1773 $\text{cm}^{-1}$ )				SOE (1736 $\text{cm}^{-1}$ )				TMA			
	$E$ (kJ/mol)	$\ln[g(\alpha)/A]$ (s)	$\ln A$ ( $\text{s}^{-1}$ )	$r$	$E$ (kJ/mol)	$\ln[g(\alpha)/A]$ (s)	$\ln A$ ( $\text{s}^{-1}$ )	$r$	$E$ (kJ/mol)	$\ln[g(\alpha)/A]$ (s)	$\ln A$ ( $\text{s}^{-1}$ )	$r$	$E$ (kJ/mol)	$\ln[g(\alpha)/A]$ (s)	$\ln A$ ( $\text{s}^{-1}$ )	$r$
0.1	79.0	-18.95	15.58	0.999	85.4	-20.85	17.48	0.999	78.6	-18.68	15.31	1.000	35.5	-7.76	4.40	0.997
0.2	83.9	-19.70	17.06	0.999	81.5	-18.81	16.18	0.993	65.4	-13.28	10.64	0.997	29.8	-5.49	2.86	0.994
0.3	78.1	-17.53	15.34	0.999	76.1	-16.81	14.62	0.993	68.2	-13.69	11.50	0.998	31.6	-5.60	3.41	0.998
0.4	74.0	-16.05	14.19	1.000	72.7	-15.55	13.69	0.994	68.3	-13.44	11.59	0.997	37.0	-6.73	4.87	0.990
0.5	72.3	-15.34	13.75	0.999	72.7	-14.56	12.98	0.996	71.6	-14.18	12.60	0.997	41.0	-7.35	5.77	0.995
0.6	71.0	-14.65	13.31	1.000	72.0	-14.88	13.55	0.999	72.1	-14.12	12.79	0.997	41.1	-6.84	5.51	0.997
0.7	70.6	-14.29	13.18	1.000	72.5	-14.78	13.67	0.999	72.6	-14.10	13.00	0.997	56.0	-10.53	9.43	0.998
0.8	69.5	-13.74	12.86	0.999	75.1	-15.22	14.34	0.998	72.7	-13.99	13.12	0.997	51.3	-8.87	7.99	0.990
0.9	68.3	-13.13	12.50	0.999									54.8	-9.65	9.03	0.991

<sup>a</sup>  $\alpha$  refers to  $\alpha_{\text{epoxy}}$ ,  $\alpha_{\gamma\text{-BL}}$ , and  $\alpha_{\text{SOE}}$  depending on the absorbance peak used and  $\alpha_{\text{TMA}}$ .  $\ln[g(\alpha)/A]$  and  $E$  were calculated on the basis of isothermal experiments by FTIR and TMA, as the intercept and the slope of the isoconversational relationship  $\ln t = \ln[g(\alpha)/A] + E/RT$ ;  $\ln A$  was calculated using kinetic model  $R_3$  and  $\ln[g(\alpha)/A]$ .

TABLE II  
Algebraic Expressions for  $f(\alpha)$  and  $g(\alpha)$  for the Kinetic Models Used

Model	$f(\alpha)$	$g(\alpha)$
A <sub>2</sub>	$2(1 - \alpha)[- \ln(1 - \alpha)]^{1/2}$	$[- \ln(1 - \alpha)]^{1/2}$
A <sub>3</sub>	$3(1 - \alpha)[- \ln(1 - \alpha)]^{2/3}$	$[- \ln(1 - \alpha)]^{1/3}$
R <sub>2</sub>	$2(1 - \alpha)^{1/2}$	$[1 - (1 - \alpha)]^{1/2}$
R <sub>3</sub>	$3(1 - \alpha)^{2/3}$	$[1 - (1 - \alpha)]^{1/3}$
D <sub>1</sub>	$1/2(1 - \alpha)^{-1}$	$\alpha^2$
D <sub>2</sub>	$-\ln(1 - \alpha)$	$(1 - \alpha)\ln(1 - \alpha) + \alpha$
D <sub>3</sub>	$3/2(1 - \alpha)^{2/3} [1 - (1 - \alpha)]^{-1/3}$	$[1 - (1 - \alpha)^{1/3}]^2$
D <sub>4</sub>	$3/2(1 - \alpha)^{1/3} [1 - (1 - \alpha)]^{-1/3}$	$(1 - 2/3\alpha)(1 - \alpha)^{2/3}$
F <sub>1</sub>	$(1 - \alpha)$	$-\ln(1 - \alpha)$
F <sub>2</sub>	$(1 - \alpha)^2$	$(1 - \alpha)^{-1}$
F <sub>3</sub>	$1/2(1 - \alpha)^3$	$(1 - \alpha)^{-2}$
Power	$2\alpha^{1/2}$	$\alpha^{1/2}$
$n + m = 2; n = 1.9$	$\alpha^{0.1} (1 - \alpha)^{1.9}$	$[(1 - \alpha)\alpha^{-1}]^{-0.9} (0.9)^{-1}$
$n + m = 2; n = 1.5$	$\alpha^{0.5} (1 - \alpha)^{1.5}$	$[(1 - \alpha)\alpha^{-1}]^{-0.5} (0.5)^{-1}$
$n = 2$	$(1 - \alpha)^2$	$-1 + (1 - \alpha)^{-1}$
$n = 3$	$(1 - \alpha)^3$	$2^{-1}[-1 + (1 - \alpha)^{-2}]$

$E$  and  $A$  we used the average of the values obtained between  $\alpha = 0.2$  and  $\alpha = 0.8$  ( $E_{\text{epoxy}} = 74.2$  kJ/mol and  $\ln A_{\text{epoxy}} = 14.24$  s<sup>-1</sup>,  $E_{\gamma\text{-BL}} = 74.6$  kJ/mol and  $\ln A_{\gamma\text{-BL}} = 14.15$  s<sup>-1</sup>,  $E_{\text{SOE}} = 70$  kJ/mol, and  $\ln A_{\text{epoxy}} = 12.17$  s<sup>-1</sup>). The same values of  $\ln A$  can be obtained from the overall values of  $E$  and the IKR of the corresponding R<sub>3</sub> model. Thus, it can be observed that the R<sub>3</sub> model accurately describes all the reactive processes. The data obtained by this methodology are similar to those obtained by isoconversional adjustment and to the experimental values. This indicates that the methodology for determining the complete kinetic triplet  $E$ ,  $\ln A$ , and  $g(\alpha)$  is correct and can be used to study other reactive systems. Other models with good regressions (Table III), but with  $T_{\text{iso}}$  values that are substantially different from the experimental temperatures, do not give good results for either  $\alpha_{\text{epoxy}}$  or  $\alpha_{\gamma\text{-BL}}$ .

For  $\alpha_{\text{epoxy}}$  and  $\alpha_{\gamma\text{-BL}}$ , where the  $T_{\text{iso}}$  values are close to the experimental temperatures, any pair of values  $E$  and  $\ln A$  of the relationship IKR can be used to simulate the curing near the  $T_{\text{iso}}$ . Figure 7 shows the logarithm of the rate constant  $\ln k$ , associated with the epoxy group, for several activation energies. The pre-exponential factors, for each  $E$ , were calculated using the relationship IKR of the R<sub>3</sub> model and  $\ln k$  using the Arrhenius equation:

$$\ln k = \ln A - \frac{E}{RT} \quad (11)$$

It can be observed that if the activation energy  $E$  varies slightly near the  $T_{\text{iso}}$  the rate constant remains practically unchanged.

An alternative to isothermal curing is nonisothermal curing in the DSC. One of the problems associated with this method is that overall curing generally pro-

vides no kinetic information about the elemental processes.

In a previous study<sup>9</sup> we determined that the enthalpy related to the opening of the oxirane ring is about 94 kJ/mol in both homopolymerization and copolymerization with  $\gamma\text{-BL}$  or SOE. On the other hand, the enthalpy associated with the homopolymerization of SOE groups is only 21 kJ/mol. Taking these values into account, and the fact that no more than 50% of SOE homopolymerizes, practically all the evolved heat in a dynamic experiment should be associated with the reactive processes in which epoxy groups participate. Therefore, the kinetics obtained from nonisothermal experiments are expected to be similar to the kinetics obtained isothermally for the epoxy groups. Figure 8 plots conversion against curing temperature for the nonisothermal curing of DGEBA with  $\gamma\text{-BL}$  at different heating rates. Using eq. (9) we determined the isoconversional parameters and then calculated the isothermal parameters of eq. (5). Table IV shows the results. From these parameters we simulated the conversion of epoxide groups, which are represented in Figure 3. The goodness of the simulation and the regressions obtained (Table IV), in addition to the fact that the nonisothermal kinetic parameters are similar to those of epoxy groups, confirm that our hypotheses are correct. When the Flynn–Wall–Ozawa method<sup>20,21</sup> was used instead of eq. (9) the results were similar.

To determine the kinetic model from nonisothermal parameters we used two different strategies. We used the Coats–Redfern method [eq. (8)] to determine  $E$  and  $\ln A$  for the different models. Table V shows all the results obtained at a heating rate of 10 K min<sup>-1</sup>. We took R<sub>3</sub> as the correct model because it is better adjusted. Some other models have good regressions but



TABLE III  
Isokinetic Parameters Obtained from the Compensation Curves for the Different Models Used<sup>a</sup>

Model	Epoxy (915 cm <sup>-1</sup> )			$\gamma$ -Butyrolactone (1773 cm <sup>-1</sup> )			SOE (1736 cm <sup>-1</sup> )			TMA					
	<i>a</i>	<i>b</i>	<i>T</i> <sub>iso</sub>	<i>a</i>	<i>b</i>	<i>T</i> <sub>iso</sub>	<i>a</i>	<i>b</i>	<i>T</i> <sub>iso</sub>	<i>a</i>	<i>b</i>	<i>T</i> <sub>iso</sub>	<i>r</i>		
A <sub>2</sub>	0.3151	-8.228	108.7	0.3078	-7.837	117.7	0.9968	0.3479	-11.31	72.7	0.9896	0.2255	-2.711	260.4	0.9965
A <sub>3</sub>	0.3833	-12.63	40.8	0.3774	-12.34	45.7	0.9888	0.3695	-12.09	52.5	0.9274	0.1961	-0.751	340.3	0.9812
R <sub>2</sub>	0.2968	-7.453	132.2	0.2954	-7.441	134.2	0.9991	0.3512	-12.08	69.5	0.9968	0.2375	-3.725	233.4	0.9985
R <sub>3</sub>	0.2886	-7.183	143.8	0.2910	-7.458	140.3	0.9993	0.3525	-12.53	68.2	0.9981	0.2421	-4.258	223.4	0.9991
D <sub>1</sub>	0.1974	0.450	336.3	0.1905	0.0651	358.4	0.9764	0.3192	-10.24	103.8	0.9316	0.2830	-6.008	152.0	0.9898
D <sub>2</sub>	0.1710	1.0384	430.4	0.1748	0.757	415.1	0.9455	0.3231	-11.02	99.2	0.9013	0.2975	-7.081	131.3	0.9893
D <sub>3</sub>	0.1375	2.2800	601.7	0.1569	0.8242	493.6	0.8832	0.3285	-12.69	93.1	0.8627	0.3162	-9.102	107.4	0.9880
D <sub>4</sub>	0.1599	0.4379	478.7	0.1688	-0.225	439.5	0.9280	0.3249	-12.57	97.2	0.8887	0.3037	-8.754	123.0	0.9890
F <sub>1</sub>	0.2706	-4.608	171.5	0.2818	-5.544	153.8	0.9984	0.3555	-11.53	65.3	0.9932	0.2523	-3.444	203.7	0.9880
F <sub>2</sub>	0.3252	-7.281	96.8	0.3678	-10.70	54.0	0.9970	0.3959	-13.05	30.8	0.9601	0.2327	-1.252	243.8	0.9840
F <sub>3</sub>	0.2106	2.0833	298.1	0.3105	-5.657	114.3	0.9679	0.4152	-13.72	16.7	0.9747	0.2974	-3.092	131.4	0.9848
Power	0.3791	-12.59	44.3	0.3665	-11.78	55.2	0.9883	0.3622	-11.84	59.1	0.9351	0.1968	-1.062	338.2	0.9844
<i>n</i> + <i>m</i> = 2;															
<i>n</i> = 1.9	0.2276	-0.827	255.5	0.2679	-3.985	175.9	0.9860	0.3682	-11.91	53.7	0.9871	0.2780	-3.931	159.6	0.9974
<i>n</i> + <i>m</i> = 2;															
<i>n</i> = 1.5	0.3218	-7.223	100.7	0.3378	-8.575	83.1	0.9977	0.3719	-11.48	50.4	0.9767	0.2291	-1.288	252.0	0.9937
<i>n</i> = 2	0.1969	1.3935	337.9	0.2505	-2.796	207.1	0.9735	0.3672	-11.98	54.5	0.9743	0.2902	-4.550	141.5	0.9966
<i>n</i> = 3	0.1217	7.4371	715.3	0.2142	0.3823	288.5	0.8783	0.3826	-12.64	41.4	0.9115	0.3377	-5.966	83.2	0.9843

<sup>a</sup> *T*<sub>iso</sub> (°C) calculated using *a* = 1/*RT*<sub>iso</sub>.

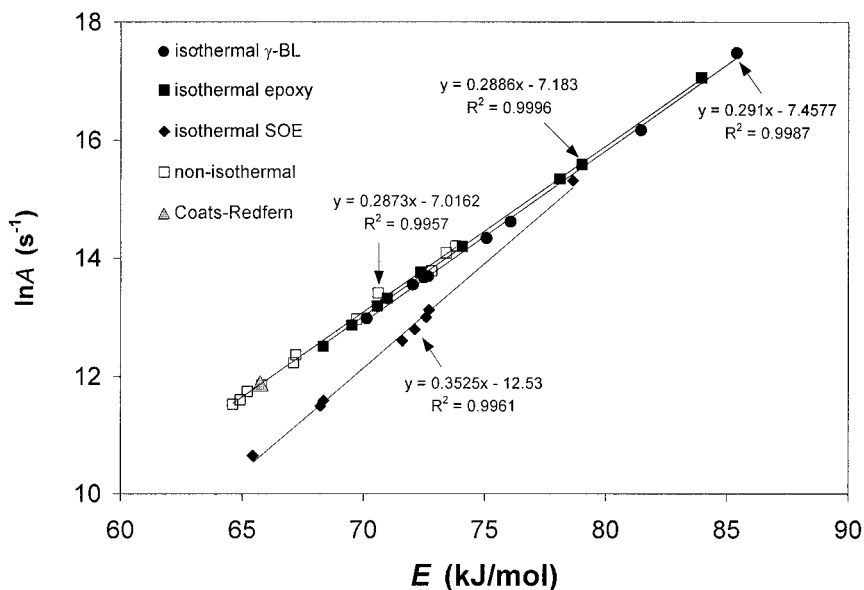


Figure 6 Isokinetic relationships (IKR) associated with each reactive group for the  $R_3$  model.

we did not consider them, given that  $E$  is quite different from that obtained isoconversionally (considered to be the true  $E$ ). If the variation in activation energy with the degree of conversion is taken into account, the kinetic model can be determined as in the isothermal case. From the isoconversional values in Table IV, we calculated the IKRs for the different models. Table V shows the results. Again the  $R_3$  model gives the best regression and the  $T_{\text{iso}}$  of 145.6°C lies in the experimental range of curing temperatures. In Table IV we can see the preexponential factors determined from

the isoconversional values by the  $R_3$  model and, in Figure 6, the agreement between the isothermal IKR for  $\alpha_{\text{epoxy}}$  and nonisothermal IKR. Moreover, we can see that the kinetic parameters determined by the Coats–Redfern method lie on the nonisothermal IKR.

Figure 3 shows the simulated conversion of epoxy groups from the  $R_3$  model and the nonisothermal values. We used the values of  $E = 66.5$  kJ/mol and  $\ln A = 12.1$  s $^{-1}$ , obtained as average values of the parameters between conversions in the range 0.2–0.8. For  $E = 66.5$  kJ/mol we obtained the same preexponential

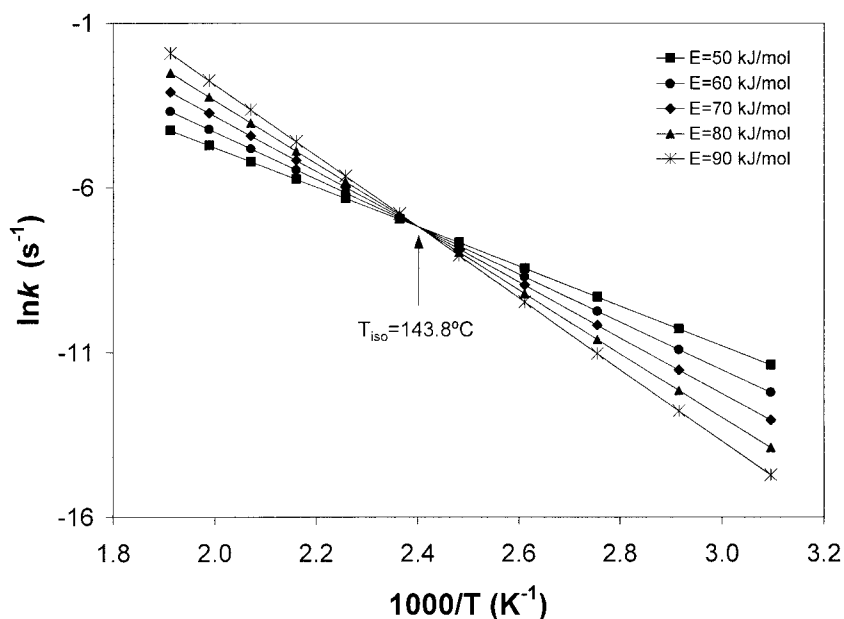
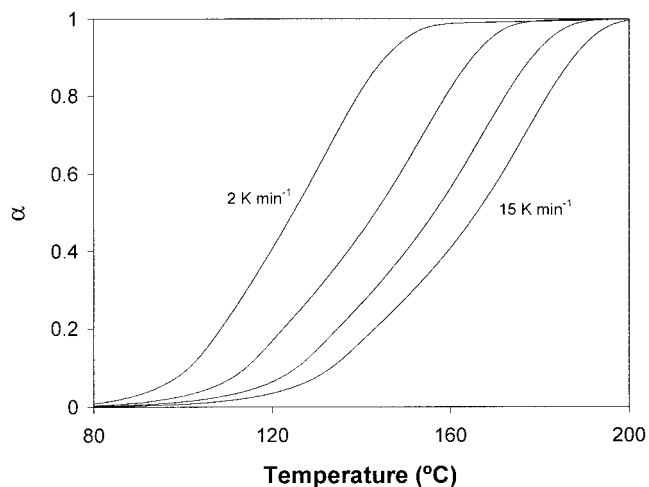


Figure 7 Plots of  $\ln k$  associated with the epoxy groups versus  $T^{-1}$  for several activation energies.



**Figure 8** Degree of conversion versus temperature, calculated according to eq. (3) for nonisothermal curing. Heating rates of 2, 5, 10, and 15 K min<sup>-1</sup>.

factor as when the IKR of the  $R_3$  model was used. Again we correctly predicted the isothermal parameters by this procedure.

In a previous study<sup>9</sup> we used TMA to measure the contraction during the curing of this type of materials. We found that there is a nondirect relationship between shrinkage and degree of conversion. This is because all the elemental processes are chemically similar but they undergo very different contractions. Specifically, the homopolymerization of DGEBA contracts by 2.4%<sup>9</sup> and the reaction of DGEBA with  $\gamma$ -BL contracts much more, as much as 11.2% for related compounds.<sup>1</sup> On the other hand, the polymerization of SOE and its copolymerization with DGEBA take place either with contractions that are almost zero or even with expansion.<sup>32</sup> Depending on the elemental reactions that occur in the different stages of curing, the material will contract to one degree or another.

Figure 9 shows the degree of contraction calculated by eq. (2) for several temperatures as a function of the curing time in the TMA. We can observe a contraction, characteristic of these systems, in two or three steps and separated by the gelation of the material ( $\alpha_{\text{TMA}} \approx 0.7$ ), which takes place with no apparent contraction.<sup>9</sup> We analyzed the kinetics of the contraction in a similar way to the curing monitored by FTIR. Table I shows the kinetic parameters of isoconversional analysis. These parameters differ from those obtained for the chemical conversions in the FTIR. In general, the activation energy increases, particularly when  $\alpha_{\text{TMA}} \geq 0.7$ . This fact could be explained by the difficulty of contracting the gelled material. Moreover, all the kinetic parameters change considerably during the curing process. These values are distributed in three different regions:  $\alpha_{\text{TMA}}$  between 0.1 and 0.3,  $\alpha_{\text{TMA}}$  between 0.4 and 0.6, and  $\alpha_{\text{TMA}}$  between 0.7 and 1. Figure

9 shows good agreement between the isoconversional kinetic parameters and experimental contractions.

To determine the kinetic model we ascertained the isokinetic relationships (Table III). Again, the most reliable model is  $R_3$ , which has an associated  $T_{\text{iso}}$  of 223.4°C. This isokinetic temperature is slightly beyond the experimental temperature range. Results for the  $R_3$  model could be better if we group the  $E$  and  $\ln A$  values in two IKRs. The first ( $a = 0.2768$ ,  $b = -5.3633$ ,  $T_{\text{iso}} = 161.5^\circ\text{C}$ , and  $r = 0.9999$ ) groups the values up to  $\alpha_{\text{TMA}} < 0.7$ . The second ( $a = 0.3085$ ,  $b = -7.8633$ ,  $T_{\text{iso}} = 116.9^\circ\text{C}$ , and  $r = 0.9996$ ) groups the values for  $\alpha_{\text{TMA}} \geq 0.7$ .

Figure 9 shows the  $R_3$  model's prediction of the contraction at 120 and 140°C. Because of the considerable change in the kinetic parameters the simulation, taking  $E$  and  $\ln A$  as constants, is not very accurate. Thus, we simulated the contraction in the three groups mentioned above, and took the following average kinetic parameters: at low contractions,  $E = 32$  kJ/mol and  $\ln A = 5.33$  s<sup>-1</sup>; at medium contractions,  $E = 38$  kJ/mol and  $\ln A = 5.38$  s<sup>-1</sup>; and at high contractions,  $E = 54$  kJ/mol and  $\ln A = 8.82$  s<sup>-1</sup> (Fig. 9). As we can see, the simulated shrinkages perfectly fit the experimental data, which confirms that the  $R_3$  model is also suitable for predicting the contraction process in this complex curing system.

## CONCLUSIONS

FTIR spectroscopy made it possible to analyze the individual elemental chemical processes that take part in a complex curing process such as the cationic crosslinking of DGEBA/ $\gamma$ -BL mixtures. In this reactive system we determined the conversions and kinetic

**TABLE IV**  
Kinetic Parameters of Nonisothermal Curing Obtained by DSC<sup>a</sup>

$\alpha$	$E$ (kJ/mol)	$\ln[AR/g(\alpha)E]$ (K s <sup>-1</sup> )	$\ln[g(\alpha)/A]$ (s)	$\ln A$ (s <sup>-1</sup> )	$r$
0.05	75.4	9.48	-18.59	14.52	0.9983
0.1	73.4	8.36	-17.45	14.08	0.9989
0.2	70.6	6.99	-16.04	13.41	0.9992
0.3	67.2	5.55	-14.55	12.36	0.9996
0.4	65.2	4.63	-13.60	11.74	0.9997
0.5	64.6	4.15	-13.10	11.52	0.9996
0.6	64.9	3.97	-12.93	11.60	0.9993
0.7	65.8	3.98	-12.95	11.85	0.9991
0.8	67.1	4.11	-13.11	12.23	0.9990
0.9	69.7	4.55	-13.58	12.96	0.9991
0.95	72.8	5.16	-14.24	13.78	0.9995

<sup>a</sup>  $\ln[AR/g(\alpha)E]$  and  $E$  were calculated on the basis of the nonisothermal DSC experiments, as the intercept and the slope of the isoconversional relationship  $\ln[\beta/T^2] = \ln[AR/g(\alpha)E] - E/RT$ ;  $\ln[g(\alpha)/A]$  was calculated on the basis of  $\ln[AR/g(\alpha)E]$  and  $E$ ;  $\ln A$  was calculated using kinetic model  $R_3$  and  $\ln[g(\alpha)/A]$ .

TABLE V  
Arrhenius Parameters Determined by the Coats–Redfern Method [Eq. (8)]<sup>a</sup>

Model	Coats–Redfern			Isokinetic relationship			
	$E$ (kJ/mol)	$\ln A$ (s <sup>-1</sup> )	$r$	$a$	$b$	$T_{\text{iso}}$	$r$
A <sub>2</sub>	30.5	3.60	0.9979	0.2809	-6.596	155.1	0.9955
A <sub>3</sub>	20.0	-0.65	0.9974	0.3860	-12.184	38.6	0.9168
R <sub>2</sub>	61.9	11.09	0.9989	0.2819	-6.326	153.7	0.9937
R <sub>3</sub>	65.7	11.88	0.9995	0.2873	-7.0162	145.6	0.9978
D <sub>1</sub>	110.5	25.02	0.9887	0.1343	3.326	622.6	0.6994
D <sub>2</sub>	129.9	31.08	0.9945	0.1267	3.398	676.3	0.5681
D <sub>3</sub>	138.3	31.43	0.9974	0.1231	2.436	704.1	0.4415
D <sub>4</sub>	128.1	28.24	0.9953	0.1253	2.087	686.9	0.5214
F <sub>1</sub>	74.1	15.58	0.9983	0.2803	-5.294	156.1	0.9933
F <sub>2</sub>	45.6	8.39	0.9083	0.4398	-14.696	0.5	0.9962
F <sub>3</sub>	98.2	24.83	0.9192	0.4407	-13.764	-0.1	0.8803
Power	22.3	-0.14	0.9823	0.3627	-9.730	58.6	0.9937
$n + m = 2; n = 1.9$	93.2	21.78	0.9900	0.3027	-6.154	124.3	0.9096
$n + m = 2; n = 1.5$	44.9	7.36	0.9971	0.3632	-9.730	58.2	0.9931
$n = 2$	104.4	24.93	0.9902	0.2875	-5.219	145.4	0.8435
$n = 3$	141.6	36.27	0.9746	0.3028	-5.584	124.2	0.6238

<sup>a</sup> Isokinetic relationships obtained from eq. (10).  $T_{\text{iso}}$  (°C) calculated using  $a = 1/RT_{\text{iso}}$ .

ics of the epoxy,  $\gamma$ -BL, and SOE. DSC, on the other hand, could not separate the elemental processes and thus provided only the global kinetics of the crosslinking.

All the elemental reactions that participated in the curing of DGEBA epoxy resins with  $\gamma$ -butyrolactone catalyzed by ytterbium triflate followed a kinetic model of the surface-controlled reaction type, R<sub>3</sub>. The reactions in which epoxy groups and/or  $\gamma$ -butyrolactone take part had a similar kinetic triplet, whereas the SOE reaction had a slightly different triplet.

Isoconversional methods made it possible to evaluate how the kinetic parameters varied with the degree

of conversion but they did not reveal the complete kinetic triplet. Using these methods in combination with the isokinetic relationships, both in the isothermal and nonisothermal curing, enabled us to determine the complete kinetic triplet [ $E$ ,  $A$ ,  $g(\alpha)$ ].

The kinetics of the shrinkage in TMA were evaluated with the same methodology as in the FTIR studies. The shrinkage also followed a type R<sub>3</sub> kinetic model, but its activation energies and preexponential factors varied considerably during the curing process because they depended heavily on the elemental chemical reactions and the physical phenomena that took place at each stage.

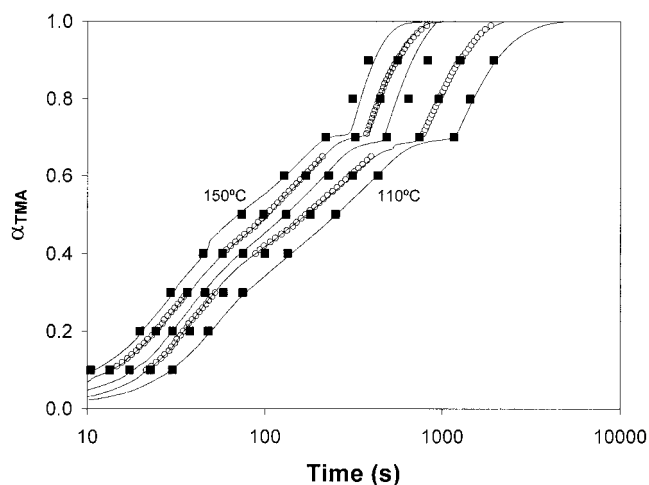


Figure 9 Experimental and simulated degrees of shrinkage versus time for samples cured in TMA at 150, 140, 130, 120, and 110°C: (—) experimental isothermal curves; (■) isoconversional isothermal data obtained by eq. (5); (○) curves obtained by using function R<sub>3</sub> and average isothermal kinetic parameters (Table I).

The authors from the UPC thank CICYT (Comisión Interministerial de Ciencia y Tecnología) for Grant MAT2000-1002-C02-02 and CICYT and FEDER for Grant PPQ2001-2764-C03-02. The authors from the URV thank CICYT, FEDER (Grant MAT2002-00291), and CIRIT (Comissió Interdepartamental de Recerca i Innovació Tecnològica) for Grant SGR 00318.

## References

- Sadhir, R. K.; Luck, M. R., Eds. *Expanding Monomers: Synthesis, Characterization and Applications*; CRC Press: Boca Raton, FL, 1992.
- Eom, Y.; Boogh, L.; Michaud, V.; Sunderland, P.; Manson, J.-A. *Polym Eng Sci* 2001, 41, 492.
- Bailey, W. J.; Sun, R. L.-J.; Katsuki, H.; Endo, T.; Iwama, H.; Tsushima, R.; Saigou, K.; Bitritto, M. M. In: *Ring-Opening Polymerization*; Saegusa, T.; Goethals E., Eds.; ACS Symposium Series 59; American Chemical Society: Washington, DC, 1977.
- Sanda, F.; Endo, T. *J Polym Sci Part A: Polym Chem* 2001, 39, 265.
- Fedtke, M.; Haufe, J.; Kahlert, E.; Müller, G. *Angew Makromol Chem* 1998, 255, 53.
- Matějka, L.; Chabanne, P.; Tighzert, L.; Pascault, J. P. *J Polym Sci Part A: Polym Chem* 1994, 32, 1447.

7. Castell, P.; Galià, M.; Serra, A.; Salla, J. M.; Ramis, X. *Polymer* 2000, 41, 8465.
8. Mas, C.; Serra, A.; Mantecón, A.; Salla, J. M.; Ramis, X. *Macromol Chem Phys* 2001, 202, 2554.
9. Mas, C.; Ramis, X.; Salla, J. M.; Mantecón, A.; Serra, A. *J Polym Sci Part A: Polym Chem* 2003, 41, 2794.
10. Ramis, X.; Cadenato, A.; Morancho, J. M.; Salla, J. M. *Polymer* 2003, 44, 2067.
11. Vyazovkin, S.; Linert, W. *Int Rev Phys Chem* 1995, 14, 355.
12. Budrugaec, P.; Homentcovschi, D.; Segal, E. *J Therm Anal Cal* 2001, 63, 457.
13. Salla, J. M.; Ramis, X.; Morancho, J. M.; Cadenato, A. *Thermochim Acta* 2002, 388, 355.
14. Zhiqiang, Z.; Bangkun, J.; Pingsheng, H. *J Appl Polym Sci* 2002, 84, 1457.
15. Fridman, H. *J Polym Sci* 1963, C6, 183.
16. Vyazovkin, S.; Sbirrazzuoli, N. *Macromol Chem Phys* 1999, 200, 2294.
17. Coats, A. W.; Redfern, J. P. *Nature* 1964, 207, 290.
18. Vyazovkin, S.; Dollimore, D. *J Chem Inform Comput Sci* 1996, 36, 42.
19. Kissinger, H. E. *Anal Chem* 1957, 29, 1702.
20. Flynn, J. H.; Wall, L. A. *J Res Natl Bur Stand A Phys Chem* 1966, 70A, 487.
21. Ozawa, T. *Bull Chem Soc Jpn* 1965, 38, 1881.
22. Ramis, X.; Salla, J. M.; Cadenato, A.; Morancho, J. M. *J Therm Anal Cal* 2003, 72, 707.
23. Ramis, X.; Salla, J. M. *J Polym Sci Part B: Polym Phys* 1997, 35, 371.
24. Linert, W. *Chem Soc Rev* 1989, 18, 477.
25. Vyazovkin, S. *Int J Chem Kinet* 1996, 28, 95.
26. Vyazovkin, S.; Wight, C. A. *Annu Rev Phys Chem* 1997, 48, 125.
27. Vyazovkin, S.; Linert, W. *J Solid State Chem* 1995, 114, 392.
28. Linert, W.; Jameson, R. F. *Chem Soc Rev* 1989, 18, 477.
29. Salla, J. M.; Cadenato, A.; Ramis, X.; Morancho, J. M. *J Therm Anal Cal* 1999, 56, 771.
30. Vyazovkin, S. *Int Rev Phys Chem* 2000, 19, 45.
31. Vyazovkin, S.; Linert, W. *Chem Phys* 1995, 193, 109.
32. Bailey, W. J.; Iwama, H.; Tsushima, R. *J Polym Sci Symp* 1976, 56, 117.